

Chapter **1**

Introduction

Abstract

In this introductory chapter, I review the properties of low-mass galaxies, with a special focus on starbursting dwarfs. The following properties are discussed in detail: i) the gas distribution and kinematics, ii) the structural parameters of the stellar component, and iii) the resolved stellar populations and the star-formation histories. Possible scenarios for the formation and evolution of dwarf galaxies are discussed. I also briefly review the main results obtained from the study of H I rotation curves of disk galaxies. Finally, I outline the structure and main goals of this Ph.D. thesis.



Figure 1.1 – Three different types of dwarf galaxies. *Left:* a prototype dwarf spheroidal (NGC 205). *Middle:* a prototype dwarf irregular (the SMC). *Right:* a prototype blue compact dwarf (I Zw 18).

1.1 A Universe of dwarf galaxies

Low-luminosity, dwarf galaxies are the most common type of galaxies in the nearby Universe (e.g. Ferguson & Binggeli 1994). Understanding their structure, formation, and evolution is a fundamental goal for astronomy and cosmology. Dwarf galaxies are usually defined as stellar systems that have B -band absolute magnitude $M_B \gtrsim -17$ ($L_B \lesssim 10^9 L_\odot$) and are more spatially extended than globular clusters (Tammann 1994). This definition includes several different types of objects, ranging from gas-rich, star-forming galaxies to gas-poor, passively-evolving ones. In the astronomical literature, the taxonomy of dwarf galaxies is vast and, to some extent, confusing (see e.g. Binggeli 1994). Here I will use a minimal nomenclature that distinguishes between 3 types of low-mass galaxies: spheroidals, irregulars, and starbursting dwarfs (or blue compact dwarfs, BCDs).

Spheroidals (Sphs) are gas-poor dwarfs that are *not* forming stars at the present epoch. They are characterized by red colors and smooth optical isophotes, thus resembling a small elliptical galaxy (see Fig. 1.1, left). For this reason, they are sometimes referred to as dwarf ellipticals (dEs) and/or dwarf lenticulars (dS0s) (e.g. Sandage & Binggeli 1984). Following Kormendy et al. (2009), I avoid this nomenclature and indicate any gas-poor dwarf as a Sph. Sphs are typically found in the proximity of massive galaxies (e.g. the satellites of the Milky Way and M31) or in galaxy clusters.

Irregulars (Irrs) are gas-rich dwarfs that are forming stars at a relatively-low rate. They are also referred to as Magellanic irregulars (Im), after the small Magellanic cloud (SMC). The name “irregular” is due to the fact that the star-formation is not organized in spiral arms, as is common for more massive gas-rich galaxies, but is scattered in several “knots” across the galaxy (see Fig. 1.1, middle). Some gas-rich dwarfs, however, can show diffuse and/or broken spiral arms, and be classified (in order of decreasing regularity) as a late-type spiral (Sd) or as a Magellanic spiral (Sm), after the large Magellanic cloud (LMC) (e.g. de Vaucouleurs 1959; Sandage & Binggeli 1984). For the sake of simplicity, I will not distinguish between Sd, Sm, and Im types, but refer to any such gas-rich, low-mass galaxy as an Irr (as in the original morphological classifications of Hubble 1926, 1927 and Lundmark 1926, 1927). Irrs are usually found in the field or in the outskirts of galaxy clusters and galaxy groups.

Starbursting dwarfs (or BCDs) are gas-rich, low-mass galaxies that are forming stars at an unusually high rate. In the literature, they are referred to with different names, often related to the observational technique used to identify the starburst. Common nomenclature includes i) amorphous dwarfs (e.g. Gallagher & Hunter 1987; Marlowe et al. 1999), as they may have peculiar morphologies dominated by a few giant star-forming regions (see Fig. 1.1, right); ii) H II galaxies (e.g. Terlevich et al. 1991; Taylor et al. 1995), as their integrated optical spectra show strong emission-lines similar to those of H II regions in spiral galaxies; and iii) blue compact dwarfs (e.g. Zwicky & Zwicky 1971; Gil

de Paz et al. 2003), since they have blue colors, high surface brightnesses, and low luminosities. I will refer to any starbursting dwarf as a BCD. BCDs are generally found in similar environments as Irrs (the field and/or the outskirts of groups and clusters), but occasionally they can be found close to massive spiral galaxies. A nearby example is the starbursting dwarf IC 10, which is a satellite of M31 and the only known BCD in the Local Group (Gil de Paz et al. 2003).

1.1.1 The Kormendy-Binggeli diagram

Starting from the mid-80's, it has become clear that dwarf galaxies are *structurally* different from other stellar systems, such as globular clusters, elliptical galaxies, and the bulges of disk galaxies (Kormendy 1985; Sandage et al. 1985; Binggeli & Cameron 1991; Bender et al. 1992; Binggeli 1994; Ferguson & Binggeli 1994). This is clearly illustrated by a diagram, firstly made by Kormendy (1985), that plots the absolute visual magnitude M_V (proxy for the total stellar mass) versus the central surface brightness μ_V (proxy for the central stellar density) for all these objects. A modern, schematic version of this diagram is shown in Fig. 1.2 (adapted from Tolstoy et al. 2009). Different stellar systems cover different regions of the plot, and follow different trends between M_V and μ_V :

- elliptical galaxies and the bulges of disk galaxies (red ellipse) lie in the top-left region of the diagram (high stellar masses and high central densities). For these objects, the central surface brightness *decreases* with luminosity (e.g. Kormendy 1985; Kormendy et al. 2009);
- the disks of spirals and lenticulars (blue ellipse) have almost constant central surface brightness $\mu_V \simeq 21.5 \text{ mag arcsec}^{-2}$ (Freeman 1970; van der Kruit & Freeman 2011), although there also exists a population of massive, low-surface-brightness (LSB) disk galaxies with $\mu_V \lesssim 23 \text{ mag arcsec}^{-2}$ (not shown in Fig. 1.2; see Bothun et al. 1997; Tully & Verheijen 1997);
- dwarf galaxies form a sequence in the central part of the diagram (blue and yellow symbols), where the central surface brightness *increases* with luminosity. The recently discovered ultra-faint dwarfs (e.g. Willman et al. 2005; Zucker et al. 2006a,b) seem to follow the same relation defined by Sphs, Irrs, and BCDs, thus the “dwarf sequence” may span more than 4 orders of magnitude in both M_V and μ_V . Note that the canonical separation between dwarfs and “classical” galaxies at $M_B = -17 \text{ mag}$ ($M_V = -16 \text{ mag}$, dashed line) also includes low-luminosity ellipticals like M32 (red pentagon), although they are structurally different objects (e.g. Wirth & Gallagher 1984; Kormendy et al. 2009);
- globular clusters (grey dots) define a distinct sequence with respect to dwarf galaxies, where μ_V increases with M_V and spans more than 4 orders

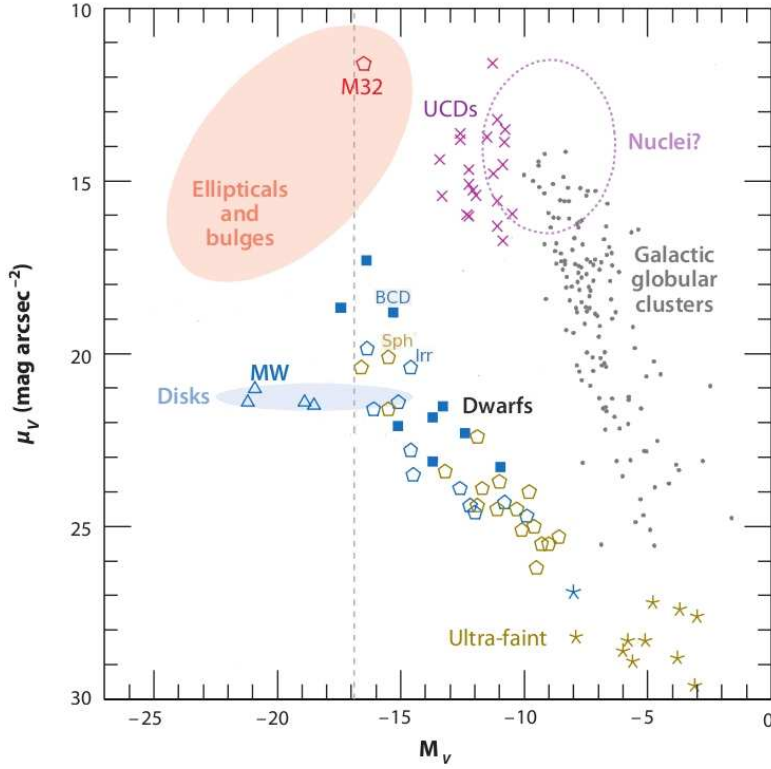


Figure 1.2 – The Kormendy-Binggeli diagram for different stellar systems (adapted from Tolstoy et al. 2009). Dwarf galaxies in the Local Group are shown by open pentagons: blue for gas-rich Irrs, yellow for gas-poor Sphs, and red for the low-luminosity elliptical M32. The recently-discovered ultra-faint dwarfs are indicated by stars. Blue squares, purple crosses, and grey points show starbursting dwarfs (BCDs), ultra-compact dwarfs (UCDs), and globular clusters, respectively. The colored ellipses show the typical location of elliptical galaxies and bulges (light-red), galactic nuclei (dashed purple), and the disks of spirals and lenticulars (light-blue). Starting from the left, the blue open triangles show M31, the Milky Way (MW), M33, and the LMC.

of magnitude. The central nuclei of galaxies (dashed, purple ellipse) may extend this trend to higher surface brightnesses;

- the ultra-compact dwarfs (UCDs), discovered independently by Hilker et al. (1999) and Drinkwater et al. (2000), lie between low-mass ellipticals and high-mass globular clusters. The nature of UCDs is currently under debate: they may simply be the extension of globular clusters to higher masses (e.g. Penny et al. 2012), or be the result of mergers of massive star-clusters (e.g. Fellhauer & Kroupa 2002; Brüns & Kroupa 2012), or be the remnant nuclei of tidally-disrupted dwarfs (e.g. Bekki et al. 2001).

In recent years, the existence of a clear distinction between ellipticals and spheroidals has been strongly debated (e.g. Jerjen & Binggeli 1997; Graham & Guzmán 2003; Gavazzi et al. 2005; Ferrarese et al. 2006). This controversy is not discussed here; I just mention that Kormendy et al. (2009) and Kormendy & Bender (2012) have confirmed the dichotomy between spheroidals and ellipticals using large samples of galaxies.

1.1.2 Evolutionary scenarios

The fact that different stellar systems follow different scaling relations between M_V and μ_V suggests that different physical mechanisms have been driving their formation and evolution (e.g. Kormendy 1985; Dekel & Silk 1986). On the other hand, the fact that Sphs, Irrs, and BCDs approximately lie in the same position of the $M_V - \mu_V$ diagram suggests that evolutionary links between them may exist (e.g. Ferguson & Binggeli 1994; Kormendy & Bender 2012). In this respect, BCDs are particularly interesting because the intense star-formation activity is a short-lived phenomenon, with typical durations of a few 100 Myr (see McQuinn et al. 2010a,b), thus they *must* evolve into a different type of galaxy as the starburst fades. The possibility of morphological transformations between dwarf galaxies is also suggested by the existence of “transition type” dwarfs, a rare class of low-mass galaxies that have intermediate properties between Sphs and Irrs/BCDs (e.g. Sandage & Hoffman 1991; Mateo 1998; Skillman et al. 2003; Dellenbusch et al. 2007, 2008). Several mechanisms (both internal and external) may transform a gas-rich dwarf (Irr or BCD) into a gas-poor Sph:

- the star-formation may consume the entire inter-stellar medium (ISM), if this is not replenished by external, fresh gas. This scenario is quite unlikely because both Irrs and BCDs generally have massive gas reservoirs, and could sustain the current star-formation rates (SFRs) for at least another Hubble time (e.g. Hunter & Elmegreen 2004);
- supernova explosions and stellar winds may blow away the entire ISM from the potential well of the galaxy (e.g. Dekel & Silk 1986). This would require a strong burst of star-formation and efficient stellar feedback (e.g. Mac Low & Ferrara 1999; Ferrara & Tolstoy 2000). In this scenario, any Irr should pass through a BCD-phase in order to evolve into a Sph;
- ram pressure stripping may remove the ISM of a dwarf as it moves through a hot medium, such as the intra-cluster medium (ICM) or the hot coronae that are believed to surround massive galaxies (e.g. Gunn & Gott 1972; Kormendy & Bender 2012; Gatto et al. 2013);
- gravitational interactions with nearby massive companions (“tidal stirring”, e.g. Mayer et al. 2006) or with the global potential of a galaxy clusters (“galaxy harassment”, e.g. Moore et al. 1998) may strip gas from

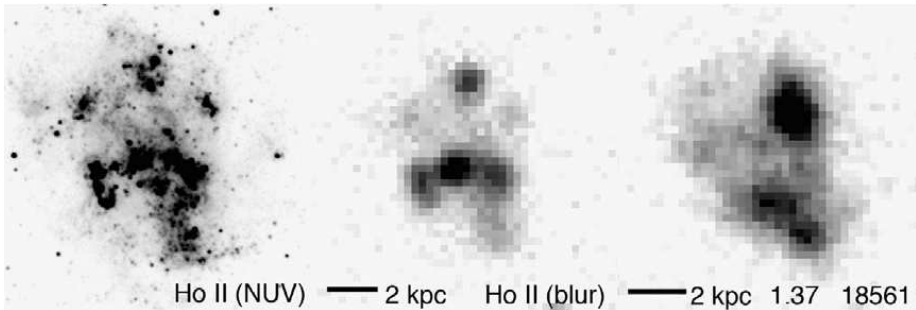


Figure 1.3 – A NUV image of the nearby starbursting dwarf Ho II (*left*), a “blurred” version of the same image (*middle*), and a HST image of the star-forming galaxy COMBO 18561 at $z \simeq 1.4$ (*right*). The blurred image of Ho II and the HST image of COMBO 18561 have the same spatial resolution (~ 780 pc) and rest-frame wavelength (~ 2400 Å). COMBO 18561 is ~ 30 times more massive than Ho II. From Elmegreen et al. (2009).

the outer parts of the galaxy and cause gas inflow towards the center. Depending on the orbits and the initial conditions, Irrs may either evolve directly into Sphs or pass through a BCD-phase.

It is also possible that a Sph may evolve into a BCD if it accretes cold gas from its surroundings, causing a sudden burst of star-formation. In particular, Silk et al. (1987) suggested that Sphs in a galaxy group may expell their ISM through stellar feedback, but this gas remains gravitationally bound to the group potential and, therefore, could fall back onto the galaxies, leading to a cyclic evolution from Sphs to BCDs and vice versa.

1.1.3 The link with the high-redshift Universe

In this section, I point out that nearby, gas-rich dwarfs, especially BCDs, show some striking similarities with more massive star-forming galaxies at high redshifts. In recent years, the development of integral field units, such as SINFONI at the ESO *Very Large Telescope* (VLT), have made it possible to discover a population of star-forming disk galaxies at $z \simeq 1 - 2$ (e.g. Förster Schreiber et al. 2006, 2009), that are thought to be the progenitors of spiral and lenticular galaxies at $z \simeq 0$ (e.g. Bournaud et al. 2007, 2009; Genzel et al. 2008). These star-forming disks have stellar masses in the range 10^{10} to $10^{11} M_{\odot}$, similar to nearby spirals and lenticulars, but show “clumpy” morphologies, similar to Irrs and BCDs. This is illustrated in Fig. 1.3 (from Elmegreen et al. 2009): the left panel shows a NUV image of Holmberg II (Ho II), a starbursting dwarf at $z \simeq 0$ (e.g. McQuinn et al. 2010b); the middle panel shows how Ho II would look like at $z \simeq 1.4$ if observed with the *Hubble Space Telescope Advance Camera for Surveys* (HST/ACS); and the right panel shows

an actual star-forming galaxy at $z \simeq 1.4$ observed with HST/ACS. Clearly, the two galaxies have very similar morphologies dominated by giant star-forming “clumps”, despite the fact that they differ in stellar mass by a factor of ~ 30 (see Elmegreen et al. 2009 for details).

The similarity between BCDs and high-redshift, star-forming galaxies is not only morphological. Several physical properties of BCDs are similar to those of high- z galaxies: i) high values of the SFR per unit area $\Sigma_{\text{SFR}} = \text{SFR}/A \simeq 0.1 - 10 \text{ M}_{\odot} \text{ yr}^{-1} \text{ kpc}^{-2}$, where A is the area of the star-forming region (e.g. Kennicutt & Evans 2012), ii) high gas fractions ($M_{\text{gas}}/L_{\text{B}} \gtrsim 1$; e.g. Salzer et al. 2002), iii) low gas metallicities ($0.2 \lesssim Z/Z_{\odot} \lesssim 0.02$; e.g. Izotov & Thuan 1999), and iv) relatively-turbulent gaseous disks, where the ratio of the rotation velocity V_{rot} to the velocity dispersion σ_{gas} ranges typically from ~ 2 to 6 (van Zee et al. 2001; Förster Schreiber et al. 2009). BCDs are, therefore, the best nearby analogs to high-redshift disk galaxies. This has led Elmegreen et al. (2009, 2012) to suggest that similar physical mechanisms may be driving the star-formation activity in both Irrs/BCDs and “clumpy” high- z disks. In particular, they argued that the irregular morphologies of these galaxies are due to gravitational instabilities in a disk that has both a high gas mass compared to the stellar mass and a high turbulent speed compared to the rotational speed. If this analogy is correct, the detailed study of nearby BCDs may shed new light also on the formation and evolution of massive disk galaxies at high redshifts.

1.2 Properties of dwarf galaxies

1.2.1 Gas distribution and kinematics

The *atomic* gas content of nearby galaxies can be investigated using radio observations of the 21-cm line. This is a hyperfine transition of the atomic hydrogen (HI), which traces gas at temperatures $T \simeq 10^2 - 10^4$ K. For massive, metal-rich galaxies, radio and sub-mm observations can be used to study also the *molecular* gas content, by targeting carbon-monoxide (CO) transition lines. This is usually not possible for low-mass galaxies, since they have low metallicities and the CO lines are often undetected (e.g. Taylor et al. 1998). Thus, I focus here on the results from HI observations.

In the past 30 years, the advent of radio interferometers like the *Westerbork Synthesis Radio Telescope* (WRST), the *Very Large Array* (VLA), and the *Giant Metrewave Radio Telescope* (GMRT) have made it possible to investigate the HI distribution and kinematics of nearby galaxies of all morphological types, ranging from disk-dominated spirals (e.g. Bosma 1978; Cayatte et al. 1990; de Blok et al. 1996; Verheijen & Sancisi 2001; Walter et al. 2008), to bulge-dominated spirals (Jore 1997; Noordermeer et al. 2005), to lenticulars and ellipticals (Serra et al. 2012). Several surveys have also been focusing on low-mass, dwarf galaxies. Swaters et al. (2002) studied the HI content

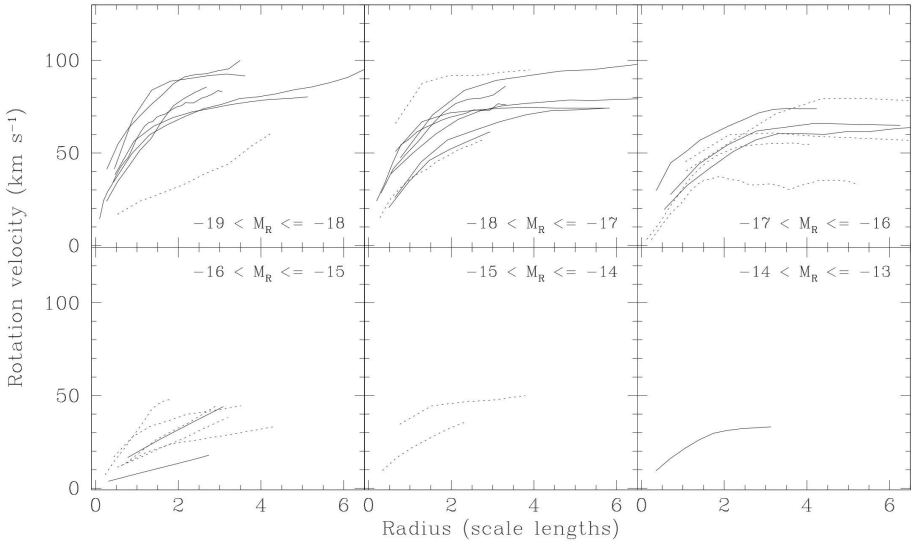


Figure 1.4 – Rotation curves of gas-rich dwarfs (from Swaters et al. 2009), with radii expressed in units of optical scale-lengths. The rotation curves are binned according to the R -band absolute magnitude of the galaxy. Full-lines indicate high-quality rotation curves, while dashed-lines indicate rotation curves of lower quality. See Swaters et al. (2009) for details.

of 73 late-type dwarfs, as part of the *Westerbork HI Survey of Spiral and Irregular Galaxies* (WHISP). Begum et al. (2008) observed 65 low-mass dwarfs (with $M_B \lesssim -13$ mag) as part of the *Faint Irregular Galaxies GMRT Survey* (FIGGS). Cannon et al. (2011) presented the *Survey of HI in Extremely Low-mass Dwarfs* (SHIELD), which focuses on dwarf galaxies at the low-mass end of the HI mass function ($M_{\text{HI}} \simeq 10^6 - 10^7 M_\odot$). Hunter et al. (2012) obtained multi-configuration VLA observations of 41 Irrs/BCDs, as part of LITTLE-THINGS (*Local Irregulars That Trace Luminosity Extremes, The HI Nearby Galaxy Survey*). Finally, Ott et al. (2012) presented VLA-ANGST (VLA *survey of ACS Nearby Galaxy Survey Treasury*), which provides HI observations of 29 nearby dwarfs that have been resolved into single stars by HST/ACS as part of the ANGST program.

These surveys, together with previous studies, have shown that gas-rich dwarfs generally have “clumpy” HI distributions, characterized by “shells”, “holes”, and localized overdensities. These structures are thought to be shaped by the star-formation activity, although the detailed connection between the HI distribution and the stellar feedback is still unclear (e.g. Warren et al. 2011). On larger spatial scales (outside the stellar component), about 30% of gas-rich dwarfs show asymmetries in their HI distribution (a so-called “morphological

Table 1.1 – Individual studies of the HI distribution and kinematics of starbursting dwarfs. The stars indicate objects that are in our galaxy sample.

Name	Other names	Reference
NGC 625*	ESO 297-G005	Cannon et al. (2004)
NGC 1569*	VII Zw 16	Stil & Israel (2002); Johnson et al. (2012)
NGC 1705*	ESO 158-G013	Meurer et al. (1998); Elson et al. (2010)
NGC 2366*	DDO 42	Hunter et al. (2001); van Eymeren et al. (2009a)
NGC 2915	ESO 037-G003	Meurer et al. (1996); Elson et al. (2013)
NGC 4670	Haro 9	Hunter et al. (1996)
NGC 4449*	UGC 7592	Hunter et al. (1998, 1999)
NGC 4861	IC 3961	van Eymeren et al. (2009b)
NGC 5253*	Haro 10	Kobulnicky & Skillman (2008); López-Sánchez et al. (2012)
NGC 2537	Mrk 86	Matthews & Uson (2008)
IC 10	UGC 192	Wilcots & Miller (1998)
I Zw 18*	Mrk 116	van Zee et al. (1998c)
I Zw 36*	Mrk 209	Viallefond & Thuan (1983); Ashley et al. (2013)
II Zw 33	Mrk 1094	Walter et al. (1997)
II Zw 40	UGCA 116	Brinks & Klein (1988)
II Zw 70/71	Mrk 829	Cox et al. (2001)
VII Zw 403*	UGC 6456	Simpson et al. (2011)
SBS 0335-052		Pustilnik et al. (2001a); Ekta et al. (2009)
VCC 144	Haro 6	Brosch et al. (1998)
FCC 35		Putman et al. (1998)

lopsidedness”, e.g. Swaters et al. 2002), which may indicate recent accretion of cold gas (Sancisi et al. 2008).

The HI kinematics of gas-rich dwarfs is generally regular and characterized by ordered rotation, although mild kinematical asymmetries are common (a so-called “kinematical lopsidedness”, e.g. Swaters et al. 2002). Swaters et al. (2009) considered 69 gas-rich dwarfs from the WHISP survey (excluding 4 interacting/merging systems) and could derive rotation curves for 62 of them ($\sim 90\%$). Figure 1.4 (from Swaters et al. 2009) shows that the rotation curves of Irrs are generally described by a nearly solid-body portion at radii $\lesssim 2 - 3$ optical scale-lengths, and a flat part in the outer regions, similarly to more massive disk galaxies (e.g. Bosma 1978; Begeman 1987). Swaters et al. (2011) used these rotation curves to investigate the distribution of mass in several Irrs; these results are discussed in Sect. 1.3.

Regarding starbursting dwarfs, many interferometric HI studies have focused on individual objects (see e.g. Table 1.1). Other authors investigated relatively-small samples of BCDs: 5 objects in Taylor et al. (1994), 5 in van Zee et al. (1998a), 8 in Simpson & Gottesman (2000), 6 in van Zee et al. (2001), 7 in Hoffman et al. 2003, 4 in Thuan et al. (2004), 4 in Ramya et al. (2011), and 8 in Most et al. (2013). These studies have shown that BCDs have centrally-concentrated gas distributions, with central HI densities $\sim 2 - 3$ times higher than in typical Irrs. Regarding the HI kinematics, some BCDs have regularly-rotating gaseous disks (e.g. Meurer et al. 1996, 1998; van Zee et al. 1998b, 2001), whereas others show complex gas kinematics (e.g. Cannon et al. 2004; Kobulnicky & Skillman 2008). To date, high-quality rotation curves and mass models have been derived for only a few BCDs (Walter et al. 1997; Elson et al.

2010; Johnson et al. 2012; Elson et al. 2013). It is unclear what fraction of BCDs have ordered/disturbed HI kinematics, and whether there is a relation between the dynamics and the starburst. In this Ph.D. thesis, I carry out the first systematic study of the HI distribution and kinematics in a relatively large sample of BCDs (18 objects), using both new and archival data.

1.2.2 Structural properties

The structural properties of galaxies can be investigated using surface brightness (SB) profiles, which are usually derived by azimuthally-averaging optical/IR images over a set of concentric ellipses. The SB profiles of Sphs, Irrs, and galaxy disks are generally well-described by an exponential law:

$$I(R) = I_0 \exp(-R/R_d), \quad (1.1)$$

where R_d is the “disk” scale-length and I_0 is the central SB in $L_\odot \text{ pc}^{-2}$. When expressed in magnitudes, this equation becomes a linear relation of the form

$$\mu(R) = \mu_0 + 1.086(R/R_d), \quad (1.2)$$

where μ_0 is the central SB in mag arcsec^{-2} . Another common fitting-function is the Sérsic profile (Sérsic 1963):

$$I(R) = I_e \exp \left\{ -b_n \left[\left(\frac{R}{R_e} \right)^{1/n} - 1 \right] \right\}, \quad (1.3)$$

where R_e is the effective radius (the radius that contains 50% of the total light), I_e is the SB at R_e (in $L_\odot \text{ pc}^{-2}$), n is the so-called Sérsic index, and b_n is a parameter that depends on n (see Ciotti 1991 and Ciotti & Bertin 1999 for details). For $n = 1$, the Sérsic profile is equivalent to an exponential with $R_d = R_e/1.678$ and $I_0 = \exp(1.678)I_e$. For $n = 4$, the Sérsic profile reduces to the De Vaucouleurs profile (de Vaucouleurs 1948), which usually describes the SB profiles of ellipticals. If the SB profiles of Irrs and Sphs are fitted with a Sérsic profile, they generally yield values of n between 0.5 and 2 (e.g. Kormendy et al. 2009).

For BCDs the situation is more complicated, as they often show complex SB profiles due to light contamination from the starburst (e.g. Papaderos et al. 1996b; Doublier et al. 1999; Cairós et al. 2001; Gil de Paz & Madore 2005). Two examples (Mkn 178 and VII Zw 403) are illustrated in Fig. 1.5 (from Papaderos et al. 2002). The SB profiles (top panels) are almost exponential in the outer regions, but they show large deviations ($\sim 1-2$ mag) in the inner parts ($R \lesssim 0.6$ kpc) due to the central starburst. The color profiles (bottom panels), indeed, are almost flat in the outer parts at $B - R \simeq 1$ mag, indicative of relatively old stellar populations, but for $R \lesssim 0.6$ kpc they show a sharp transition towards blue colors, indicative of young stellar populations.

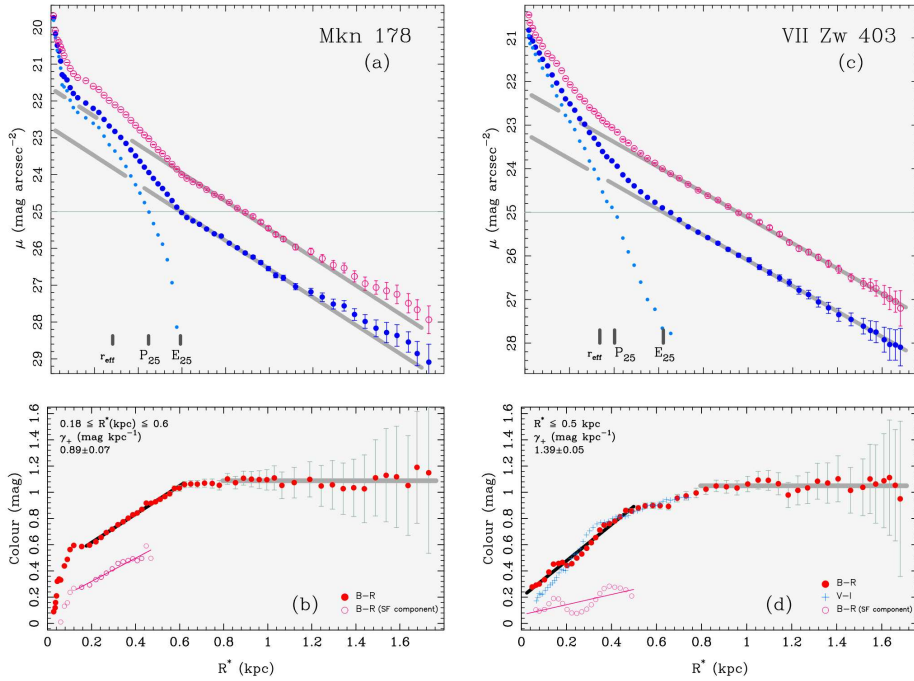


Figure 1.5 – Photometric structure of two BCD prototypes (from Papaderos et al. 2002): Mkn 178 (*left*) and VII Zw 403 (*right*). *Top*: SB profiles in the B -band (blue dots) and in the R -band (purple circles). The grey lines show exponential fits to the outer parts of the SB profiles, while the filled-cyan points are obtained by subtracting the exponential component from the B -band SB profile. The isophotal radii at $\mu_B = 25 \text{ mag arcsec}^{-2}$ are indicated for both the exponential component (E_{25}) and the “plateau” component due to the starburst (P_{25}). The effective radii is also indicated. *Bottom*: Color profiles. Red dots and cyan crosses show the $B - R$ and $V - I$ colors, respectively. The purple circles show the $B - R$ color of the starburst component. The steepness of the $B - R$ color profile (γ_+) is given to the top-left. See Papaderos et al. (2002) for details.

To compare the structural properties of BCDs with those of Sphs and Irrs, several authors (e.g. Papaderos et al. 1996b; Marlowe et al. 1999; Gil de Paz & Madore 2005) have fitted exponential and/or Sérsic profiles to the outer parts of the SB profiles of BCDs (see grey lines in Fig. 1.5), which are thought to probe their underlying, old stellar components. The extrapolated values of μ_0 , R_d , and M_{old} (the total magnitude of the old stellar component) have then been used to build $M_{\text{old}} - \mu_0$ and $M_{\text{old}} - R_d$ plots (see Fig. 1.6, adapted from Papaderos et al. 2002). According to these studies, the old stellar component of BCDs generally has higher central SB and smaller scale-length than typical Sphs and Irrs of the same luminosity. This may indicate that the evolution from a BCD to an Irr/Sph is not straightforward, possibly requiring a redistribution of

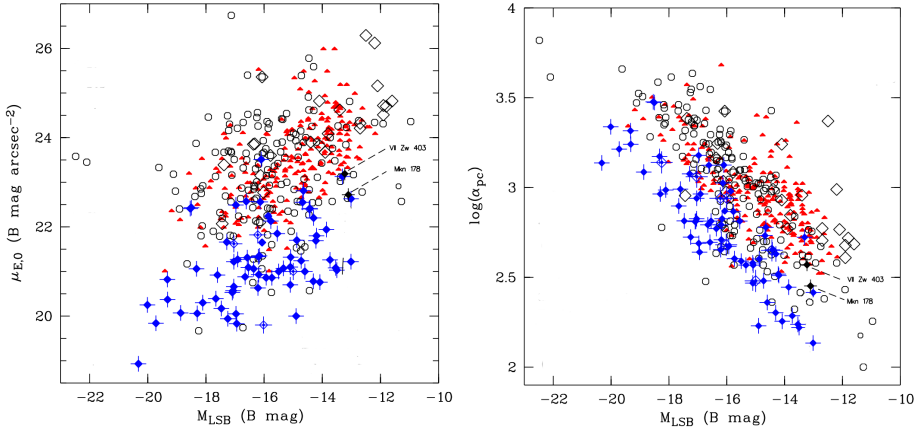


Figure 1.6 – Comparison between the structural properties of the *old* stellar component of BCDs (blue dots) with those of Sphs (red triangles) and Irrs (open circles and open diamonds). In this figure (adapted from Papaderos et al. 2002), the “disk” scale-length R_d (in pc) is indicated as α_{pc} , while the absolute magnitude of the old stellar component M_{old} is indicated as M_{LSB} . The dashed lines show the location of the two BCDs in Fig. 1.5.

the stellar mass (e.g. Papaderos et al. 1996a). Intriguingly, the central SB of the old stellar component of BCDs is, on average, ~ 21 B mag arcsec $^{-2}$, similarly to high-surface-brightness (HSB) disk galaxies (e.g. Freeman 1970; van der Kruit & Freeman 2011). Other authors (Caon et al. 2005; Micheva et al. 2013), however, found that the old stellar components of BCDs have values of μ_0 and R_d that are comparable with those of Irrs and Sphs, and argued that evolutionary links between these types of dwarfs are possible. This controversy is likely due to the intrinsic difficulty in obtaining accurate structural parameters for starbursting dwarfs. BCDs often have very irregular morphologies and the young stars may dominate the integrated light over a vast portion of the galaxy. In addition, the values of μ_0 and R_d depend on the fitted radial range of the SB profile; the selection of an optimal radial range is not always obvious, and different choices may lead to rather different results.

In this Ph.D. thesis, I tackle this problem using a different approach: I quantify the central mass density of BCDs, Irrs, and Sphs using rotation curves, that directly trace the distribution of the total dynamical mass (including stars, gas, and dark matter). This allows to put solid dynamical constraints on the evolution of dwarf galaxies.

1.2.3 Stellar Populations & Star-Formation Histories

In the past 20 years, the advent of HST has made it possible to resolve nearby galaxies into single stars and to study their stellar content in unprecedented

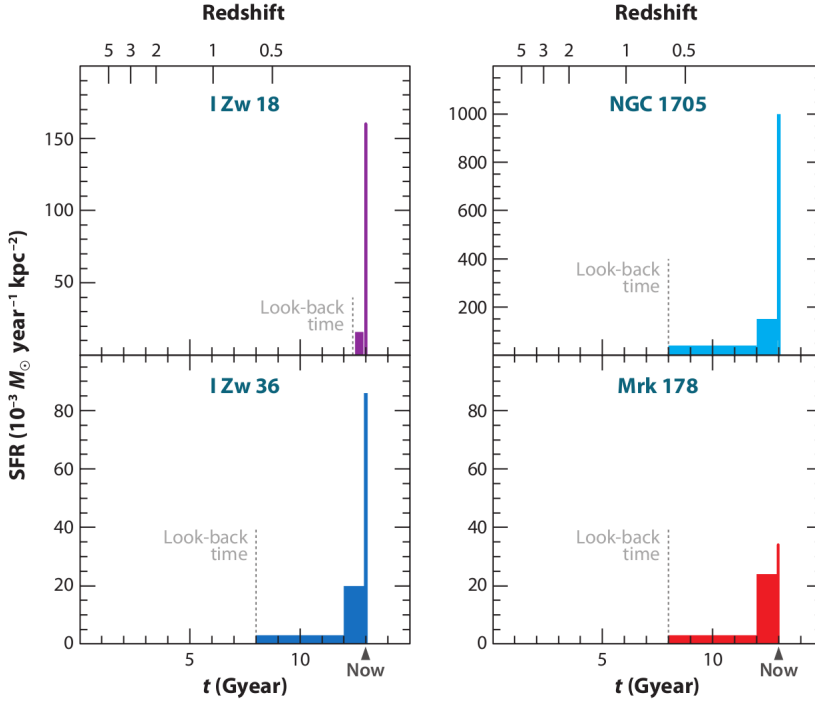


Figure 1.7 – Star-formation histories of 4 BCDs (from Tolstoy et al. 2009). The dashed, grey lines show the look-back time that can be reached by the HST photometry.

detail. Color-magnitude diagrams (CMDs) of the resolved stellar populations have been derived for several galaxies, both inside and outside the Local Group (e.g. Tolstoy et al. 2009; Dalcanton et al. 2009). In addition, the development of the synthetic CMD method (e.g. Tosi et al. 1991; Dolphin 2002) have made it possible to derive detailed star-formation histories (SFHs), i.e. the variation of the galaxy SFR over cosmic time. For details about the synthetic CMD method, I refer to Tolstoy et al. (2009) and Cignoni & Tosi (2010). Briefly, this method creates theoretical CMDs via a Monte-Carlo-based extraction of stars from a given set of evolutionary tracks, taking into account photometric errors, incompleteness, and the effects of stellar crowding. For a given metallicity, initial mass function (IMF), and binary fraction, the method can recover the SFR at different epochs, by comparing the synthetic CMDs with the observed one through a likelihood analysis to find the best-fit solution. In the following, I briefly review the results found for dwarf galaxies, with a special focus on starbursting dwarfs.

The SFHs of dwarf galaxies in the Local Group are generally complex and inconsistent with simple models, such as a single burst, exponentially declining

SFRs, or constant SFRs. They also show a great variety of shapes and SFR values (e.g. Tolstoy et al. 2009). A striking result is that only a few Sphs in the Local Group have experienced a burst of star-formation at early times and then stopped forming stars. Many of them, instead, show extended or recurrent star-formation activity, see e.g. Carina (Hurley-Keller et al. 1998) and Fornax (de Boer et al. 2012). This implies that many Sphs were gas-rich in the recent past and, if observed only ~ 1 -2 Gyr ago, would have been classified as Irrs or BCDs. Similar results have been found by Weisz et al. (2011), which studied the SFHs of 60 dwarfs *outside* the Local Group and concluded that the mean SFHs of Irrs and Sphs are similar over most of the cosmic time, and begin to diverge only a few Gyr ago.

When one compares the SFHs of different galaxies, a major complication is that the accuracy and the time resolution depend on the photometric depth of the CMDs and, thus, on the galaxy distance. As a result, the SFHs of Sphs and Irrs in the Local Group can be traced back to ~ 13 Gyr ago (e.g. Tolstoy et al. 2009), whereas those of BCDs (which are typically at distances $D \gtrsim 2$ Mpc) can be accurately traced only over the last ~ 1 Gyr and are quite uncertain at earlier epochs, where one can just obtain an average value of the SFR (see Fig. 1.7, from Tolstoy et al. 2009). Despite this complication, studies of the resolved stellar populations of BCDs have reached the following conclusions:

- all BCDs observed so far contain old stars with ages $\gtrsim 1$ Gyr. This is true also for the most metal-poor galaxies, such as I Zw 18 (e.g. Aloisi et al. 2007), which were once considered “young” galaxies undergoing their first burst of star-formation (Searle & Sargent 1972; Izotov & Thuan 2004);
- BCDs show no evidence for long quiescent periods in their SFHs, but have so-called “gasy” SFHs (Tosi 2004), characterized by long periods of moderate star-formation activity (similar to Irrs) and intense bursts;
- the starbursts correspond to an increase in the SFR by a factor of 2 to 20 with respect to the past, average SFR. This enhanced level of star-formation is sustained for hundreds of Myr with variations on smaller timescales (McQuinn et al. 2010a,b);
- the spatial distribution of the star-formation can vary across the galaxy during the starburst. In some cases, the star-formation remains concentrated towards the center, but in other cases it is strongly off-centered or widespread across the entire galaxy body (McQuinn et al. 2012).

Another important aspect of these CMD studies is that they provide a direct measure of the total stellar mass of a galaxy. This is obtained by integrating the SFH over the Hubble time and assuming that a fraction of this mass (typically 30%) has been returned to the ISM by supernovae and stellar winds.

1.3 Galaxy Dynamics

1.3.1 Basic background

In the early 70's, Ostriker & Peebles (1973) found that stellar disks are unstable against bar-like modes, and speculated that spherical haloes of unseen, dark matter (DM) must surround spiral galaxies in order to stabilize the disk. A few years later, it was found that the HI rotation curves of spiral galaxies remain flat *outside* the stellar component (e.g. Bosma 1978) and do not fall off as expected given the distribution of visible mass (e.g. Casertano 1983), providing observational support to the hypothesis of DM haloes (see Sanders 2010 for a historical review). Nowadays, DM is the backbone of theories of galaxy formation (see Sect. 1.4 for details). I mention, however, that the “mass discrepancies” observed in galaxies can also be explained empirically by alternative models, such as the Modified Newtonian Dynamics (MOND) proposed by Milgrom (1983, see Famaey & McGaugh 2012 for a review).

For gas-rich galaxies, HI rotation curves are the ideal tool to investigate the distribution of mass because i) the HI disk usually is dynamically cold (i.e. random motions give negligible dynamical support), thus its rotation velocity directly traces the gravitational potential, and ii) the HI disk extends far outside the stellar component, probing regions that are clearly dominated by DM (see Fig. 1.8). Other possible dynamical tracers are the ionized gas (observed using inter-stellar recombination lines such as the H α line) and the molecular gas (observed using transition lines of CO and other species), but they only probe the gravitational potential within the stellar component. For gas-poor galaxies, instead, the mass distribution can be investigated using stellar kinematics, which is studied by fitting the stellar absorption-lines in integrated optical/NIR spectra or, for nearby galaxies in the Local Group, by measuring the radial velocities of individual stars. In the following, I focus on results from HI observations of gas-rich galaxies.

1.3.2 The disk-halo degeneracy

Assuming that a galaxy is axisymmetric and in equilibrium, the radial force $F(R)$ in the galaxy midplane at the galactocentric radius R is given by

$$F(R) = \frac{\partial \Phi}{\partial R} = -\frac{V_{\text{circ}}^2}{R}, \quad (1.4)$$

where Φ is the gravitational potential and V_{circ} is the circular velocity. The force $F(R)$ is given by the sum of the gravitational contributions from 3 main mass components: stars, gas, and DM. Thus, V_{circ} can be written as

$$V_{\text{circ}} = \sqrt{V_*^2 + V_{\text{gas}}^2 + V_{\text{DM}}^2}, \quad (1.5)$$

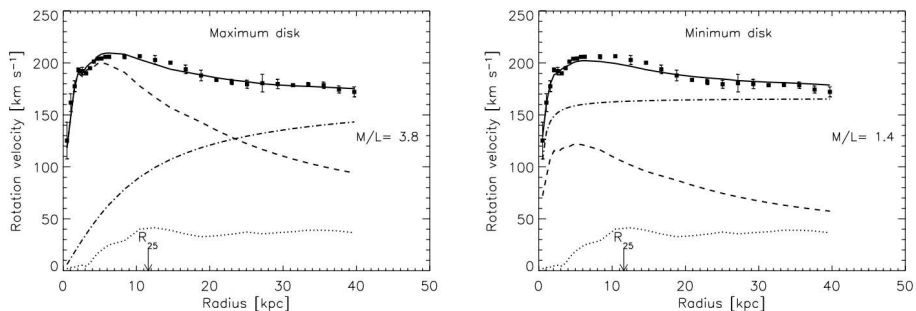


Figure 1.8 – Mass models for the HSB spiral galaxy NGC 5055, that illustrate the disk-halo degeneracy (from Battaglia et al. 2006). Squares show the observed rotation curve. Dotted, dashed, and dash-dotted lines show, respectively, the contributions due to gas, stars, and dark matter. The full line shows the resulting, total rotation curve. The left-panel shows a *maximum-disk* model, while the right-panel shows a *minimum-disk* model, where the contribution of the dark matter halo is maximized. The stellar mass-to-light ratio is in the optical F -band. The optical radius R_{25} (where $\mu = 25$ B mag arcsec $^{-2}$) is indicated. Note that only the maximum-disk model can reproduce the small feature at $R \simeq 2$ kpc and the gentle decline of the rotation velocity for $R \gtrsim 10$ kpc.

where V_* , V_{gas} , and V_{DM} are, respectively, the contributions by the stars, gas, and DM. If the galaxy does not have a significant bulge component, V_* is usually calculated assuming that the stars reside in a disk and using the observed SB profile, scaled by a given value of the stellar mass-to-light ratio (M_*/L). Similarly, V_{gas} is calculated assuming a thin disk and using the observed HI surface density profile, scaled by a factor of 1.33 to take into account the contribution of Helium. For details about the derivation of V_{circ} for a flattened mass distribution, I refer to Binney & Tremaine (1994). Finally, V_{DM} is calculated assuming a given density profile for the DM halo, that generally has 2 free parameters: a scale length and a characteristic density. This component is often assumed to have spherical symmetry, thus the Newton’s theorem can be applied.

The stellar mass-to-light ratio generally is an additional free parameter of the mass model, because direct determinations of M_*/L are rarely available. The value of M_*/L is expected to vary from galaxy to galaxy, due to differences in stellar populations, metallicities, and dust attenuation. Attempts have been made to estimate the value of M_*/L from integrated colors by using stellar populations synthesis (SPS) models (e.g. Bell & de Jong 2001), but a large number of assumptions needs to be made about the SFH, the IMF, the metallicity, the dust attenuation, and the binary fraction. As a consequence, the stellar masses from SPS models are very uncertain for galaxies with complex SFHs.

In the mid-80’s, van Albada et al. (1985) showed that different combinations of M_*/L and of the DM-halo parameters give equally good fits to the observed rotation curve, leading to large uncertainties in the final mass model. This is the so-called “disk-halo degeneracy” (see Fig. 1.8). The *maximum disk hypothesis* was then introduced (van Albada & Sancisi 1986): the contribution of the stellar disk is maximized, thus the amount of DM is minimized. For HSB disk galaxies (with $\mu_0 \simeq 21.5$ B mag arcsec $^{-2}$), maximum-disk models can explain the dynamics in the central parts with reasonable values of M_*/L and, in many cases, reproduce detailed features observed in the rotation curve (e.g. Kent 1987; Palunas & Williams 2000; see Fig. 1.8). This suggests that either the baryons dominate the dynamics in the inner parts, or DM closely follows the distribution of light (Sancisi 2004). For low-luminosity and LSB galaxies (with $\mu_0 \gtrsim 23$ B mag arcsec $^{-2}$), a maximum-disk solution can still reproduce the observed rotation curve in the central parts, but it often requires very high values of M_*/L that are difficult to reconcile with SPS models (e.g. de Blok et al. 2001; Swaters et al. 2011), leading to the interpretation that low-luminosity and LSB galaxies are dominated by DM at all radii. Studies of the stellar kinematics of Sphs in the Local Group (e.g. Tolstoy et al. 2009; Wolf et al. 2010) also support the picture that dwarf galaxies are strongly dominated by DM.

Recently, the DiskMass survey (Bershady et al. 2010) has estimated the values of M_*/L in a sample of 46 face-on spiral galaxies by measuring the stellar velocity dispersion perpendicular to the disk. They found that galaxy disks are generally sub-maximal and contribute only 40%–70% to the rotational velocity within the stellar disk (Bershady et al. 2011; Martinsson et al. 2013). In Chapter 3 and Chapter 4 of this thesis, I will break the disk-halo degeneracy using a different approach: I will use the values of M_* obtained by HST studies of the resolved stellar populations, under different assumptions for the IMF. In Chapter 7, I will also quantify the coupling between luminous and dynamical mass in the central parts of galaxies by measuring the inner circular-velocity gradient $d_R V(0)$ for a sample of spiral and irregular galaxies with high-quality rotation curves.

1.4 Dwarf galaxies in a Λ CDM cosmology

According to the Λ cold dark matter (Λ CDM) cosmological model, the mass-energy of the Universe is constituted by $\sim 26\%$ of dark matter, $\sim 70\%$ of dark energy, and only 4% of ordinary baryonic matter. This model provides remarkable fits to the baryon acoustic power spectrum at $z \simeq 1000$, as derived from observations of the cosmic microwave background (e.g. Komatsu et al. 2009; Planck Collaboration 2013), and of the galaxy power spectrum at $z \simeq 0$, as derived from large galaxy surveys (e.g. Tegmark et al. 2004). The nature of dark matter and dark energy, however, is still not understood. Dark matter is believed to consist of non-relativistic (“cold”), non-baryonic particles, that

interact predominantly through gravity. Indirect evidence for the existence of DM comes from dynamical studies of galaxies and galaxy clusters, as well as gravitational lensing (see Courteau et al. 2013 for a recent review). However, a direct detection of DM candidates by laboratory experiments, as well as an indirect detection by space detectors, is still lacking (e.g. Frenk & White 2012).

In the Λ CDM framework, the formation of large-scale structures, such as filaments and voids, is well-understood by the growth of primordial density perturbations through gravitational forces, mostly due to non-baryonic DM (see Frenk & White 2012 for a review). Galaxies are thought to form by the cooling and collapse of primordial gas into DM haloes, that progressively grow in mass and size by hierarchical merging (e.g. White & Rees 1978; White & Frenk 1991). The details of galaxy formation, however, are not well-understood, because complex baryonic physics (e.g. gas cooling, star-formation, stellar feedback, etc.) plays a major role. In the last years, there has been a substantial increase in the complexity of numerical simulations, which are now able to include several baryonic processes (e.g. Springel & Hernquist 2003; Schaye et al. 2010). Here I briefly discuss two main aspects of galaxy formation in a Λ CDM Universe, that are relevant for our investigation of starbursting dwarfs: i) the hot/cold modes of gas accretion, and ii) the effect of stellar feedback in driving the formation and evolution of dwarf galaxies.

The canonical “hot-mode” of gas accretion (White & Rees 1978; Fall & Efstathiou 1980) dictates that, when primordial gas falls into the DM halo, it is shock-heated to the virial temperature of the potential well $T_{\text{vir}} = 10^6 (V_{\text{circ}}/168 \text{ km s}^{-1})^2 \text{ K}$ and forms a hot corona of collisionally-ionized gas in quasi-hydrostatic equilibrium with the DM. Subsequently, the gas radiates its thermal energy, loses its pressure support, settles into a rotationally-supported disk, and forms stars (e.g. White & Frenk 1991; Kauffmann et al. 1993). In recent years, however, several theoretical studies have suggested that cold streams of gas can flow along cosmic filaments and reach the central parts of the DM halo, feeding the star formation without being heated to the virial temperature. This is the so-called “cold-mode” of gas accretion (e.g. Birnboim & Dekel 2003; Kereš et al. 2005). According to cosmological hydrodynamical simulations, the “hot mode” dominates the gas accretion rate in massive galaxies (baryonic masses $M_{\text{bar}} \gtrsim 10^{10} M_{\odot}$), while the “cold mode” dominates in low-mass galaxies and might still take place at $z \simeq 0$ in low-density environments (Kereš et al. 2005). Thus, isolated dwarf galaxies in the nearby Universe are prime locations to search for cold gas accretion and test the predictions of this scenario.

When cosmological simulations are compared with observations, several discrepancies emerge. For dwarf galaxies, the main issues are the following:

- bulgeless disk galaxies, which constitute the vast majority of galaxies with $V_{\text{circ}} \lesssim 100 \text{ km s}^{-1}$, are not easily reproduced by simulations (the so-called “angular momentum problem”, see e.g. Thacker & Couchman 2001);

- the central “cusps” of DM haloes, found in N-body simulations (e.g. Navarro et al. 1996), are not observed in actual dwarf galaxies (the so-called “cusp-core problem”, see e.g. de Blok et al. 2001; Oh et al. 2011);
- the number density of low-mass galaxies is overpredicted by N-body simulations by at least one order of magnitude (the so-called “missing satellites problem”; see e.g. Kauffmann et al. 1993; Kravtsov 2010).
- the baryonic Tully-Fisher relation (BTFR), a fundamental scaling-relation between the total baryonic mass of a galaxy and its circular-velocity along the flat part of the rotation curve, has an observed slope of ~ 4 (McGaugh et al. 2000; Verheijen 2001; McGaugh 2005), whereas Λ CDM models with a *constant* baryonic fraction in the disk predict a slope of ~ 3 (e.g. McGaugh 2012). This suggests that galaxies with lower circular velocities should systematically have lower baryonic fractions within their disks and, thus, be progressively more and more dominated by DM. Despite the exact value of the slope, the fact that HSB and LSB galaxies appear to have different baryonic fractions within their disks but can be found *on the same position* of the BTFR (de Blok & McGaugh 1996; Tully & Verheijen 1997) is another major challenge for the Λ CDM model.

These discrepancies are generally explained by invoking complex physical processes involving baryons, in particular strong feedback from supernovae and stellar winds, that *might* be able to expell large amounts of gas from the low potential wells of dwarf galaxies (e.g. Dekel & Silk 1986). According to recent simulations, strong supernova feedback *might* have the following effects: i) prevent the formation of a bulge by the removal of low-angular-momentum gas (e.g. Governato et al. 2010; Brook et al. 2011); ii) turn a DM “cusp” into a “core” (e.g. Governato et al. 2012); iii) suppress star-formation in low-mass DM haloes, explaining the “missing satellites problem” (e.g. Okamoto et al. 2010; Sawala et al. 2013); and iv) reduce the baryonic fraction in low-mass galaxies, reproducing the BTFR (e.g. Stringer et al. 2012; Vogelsberger et al. 2013). It is unclear, however, whether the strong stellar feedback assumed in these simulations is really taking place in dwarf galaxies. Dynamical studies of nearby starbursting dwarfs are, therefore, very important to constrain the real efficiencies of these baryonic processes.

1.5 This Ph.D. Thesis

1.5.1 Open questions

In this Ph.D. thesis, I investigate the HI distribution and kinematics of starbursting dwarf galaxies. I consider 18 nearby galaxies that satisfy two criteria: i) they have been resolved into single stars by HST and high-quality SFHs are available, and ii) the SFHs show an increase in the recent SFR by a

factor $\gtrsim 3$ with respect to the past, average SFR. This allows the identification of a representative sample of nearby starbursting dwarfs (see Chapter 4 for details). A detailed study of these objects allows addressing the following issues.

What triggers the starburst in BCDs?

The mechanisms that trigger the starburst in BCDs are not understood. Tidal interactions and galaxy mergers have been proposed as external triggers (e.g. Bekki 2008), but optical studies of the environment of BCDs have led to contradictory results (e.g. Telles & Maddox 2000; Pustilnik et al. 2001b; Noeske et al. 2001). HI studies of individual BCDs have shown that, in several cases, interactions/mergers between gas-rich dwarfs (e.g. Cox et al. 2001; Ekta et al. 2009) or cold gas accretion from the IGM (e.g. López-Sánchez et al. 2012) might be important, but other BCDs seem relatively unperturbed and isolated (e.g. Elson et al. 2010; Simpson et al. 2011). In this Ph.D. thesis, I carry out a systematic HI study of a relatively-large sample of BCDs, attacking the problem in two ways: i) high-resolution HI data are used to study the internal dynamics and the possible link with the starburst, while ii) low-resolution HI data, that are sensitive to the diffuse emission, are used to investigate the large-scale HI distribution and the possible role of external triggers. In particular, the information provided by the SFHs allows comparing the dynamical timescales with the starburst timescales, and studying the detailed link between HI morphology and starburst activity.

What is the dark matter content of BCDs?

The DM content of BCDs is largely unknown. To date, high-quality rotation curves and mass models have been derived for only a few BCDs, leading to contradictory results. Elson et al. (2010, 2013) studied the HI kinematics of NGC 2915 and NGC 1705, and argued that these two BCDs are dominated by DM at all radii (see also Meurer et al. 1996, 1998). On the contrary, Walter et al. (1997) and Johnson et al. (2012) studied the starbursting dwarfs II Zw 33 and NGC 1569, respectively, and concluded that there is no need for DM to explain their inner kinematics. These discrepancies may be due to the following reasons: i) the HI kinematics of BCDs is often complex and several effects can complicate the data analysis, such as the “clumpy” HI distribution, the relatively-high ratio between HI rotation velocity and velocity dispersion, and possibly non-circular motions; ii) it is generally difficult to estimate the stellar masses of BCDs using optical colors and stellar populations models, since the starburst may increase the total luminosity by $\sim 1-2$ mag. In this Ph.D. thesis, I tackle these issues as follows: i) I study the HI kinematics using state-of-the-art 3D disk models, that take into account the effects of the gas distribution, velocity dispersion, and non-circular motions; and ii) I use the stellar masses

provided by the HST studies of the resolved stellar population to break the disk-halo degeneracy.

What are the progenitors and descendants of BCDs?

As discussed in Sect. 1.2.2, it is unclear whether there are evolutionary connections between BCDs and other types of dwarfs. There are indications that the old stellar component of BCDs generally has a higher μ_0 and smaller R_d than typical Irrs and Sphs (e.g. Papaderos et al. 1996b; Gil de Paz & Madore 2005), but the light contamination from the starburst complicates the analysis of optical images and SB profiles. Using HI observations, van Zee et al. (2001) suggested that BCDs have a higher central concentration of mass (gas, stars, and DM) than Irrs of similar luminosities, although they did not derive accurate rotation curves. In this Ph.D. thesis, I use high-quality rotation curves to directly quantify the central dynamical mass density in BCDs. The comparison with typical Irrs and rotating Sphs puts strong dynamical constraints on the properties of the progenitors and descendants of BCDs.

1.5.2 Thesis outline

The structure of this Ph.D. thesis is as follows.

In Chapters 2 and 3, I present a detailed study of two BCD prototypes: I Zw 18 and UGC 4483. I describe in detail several 3D disk models, that are used to derive rotation curves and estimate non-circular motions. The rotation curves are then decomposed into luminous and dark matter components, and compared with those of typical Irrs of similar dynamical mass.

In Chapter 4, I describe the full sample of 18 BCDs and present HI datacubes at relatively-high spatial resolutions. These are used to investigate the distribution and kinematics of the high-column-density gas associated with the stellar body of BCDs. For galaxies with relatively-regular HI kinematics, I derive rotation curves and estimate baryonic fractions. In Appendix 4.C, I also present an optical-HI atlas that illustrates the high-resolution HI data.

In Chapter 5, I compare the dynamical properties of BCDs with those of Irrs and rotating Sphs. For these galaxies, the central dynamical mass density (gas, stars, and DM) is estimated using the inner circular-velocity gradient $d_R V(0) \simeq V_{R_d}/R_d$, where R_d is the “disk” scale length. I show that V_{R_d}/R_d correlates with several properties of dwarf galaxies. In light of these new results, several scenarios for the evolution of dwarf galaxies are discussed.

In Chapter 6, I present HI datacubes at low spatial resolutions, which are used to study the diffuse HI emission on large scales. This provides clues to the mechanism that triggers the starburst in BCDs. I also investigate the nearby environment of the 18 objects in our sample.

In Chapter 7, I extend the investigation of the inner circular-velocity gradient $d_R V(0)$ to more massive galaxies. I show that, for spiral and irregular galaxies,

$d_R V(0)$ strongly correlates with the central surface brightness. This is a scaling relation for disk galaxies.

In Chapter 8, I draw my conclusions and discuss prospects for future research.

References

- Aloisi, A., Clementini, G., Tosi, M., et al. 2007, *ApJL*, 667, L151
- Ashley, T., Simpson, C. E., & Elmegreen, B. G. 2013, *AJ*, 146, 42
- Battaglia, G., Fraternali, F., Oosterloo, T., & Sancisi, R. 2006, *A&A*, 447, 49
- Begeman, K. 1987, PhD thesis, University of Groningen, NL
- Begum, A., Chengalur, J. N., Karachentsev, I. D., Sharina, M. E., & Kaisin, S. S. 2008, *MNRAS*, 386, 1667
- Bekki, K. 2008, *MNRAS*, 388, L10
- Bekki, K., Couch, W. J., & Drinkwater, M. J. 2001, *ApJL*, 552, L105
- Bell, E. F. & de Jong, R. S. 2001, *ApJ*, 550, 212
- Bender, R., Burstein, D., & Faber, S. M. 1992, *ApJ*, 399, 462
- Bershady, M. A., Martinsson, T. P. K., Verheijen, M. A. W., et al. 2011, *ApJL*, 739, L47
- Bershady, M. A., Verheijen, M. A. W., Swaters, R. A., et al. 2010, *ApJ*, 716, 198
- Binggeli, B. 1994, in *European Southern Observatory Conference and Workshop Proceedings*, Vol. 49, *European Southern Observatory Conference and Workshop Proceedings*, ed. G. Meylan & P. Prugniel, 13
- Binggeli, B. & Cameron, L. M. 1991, *A&A*, 252, 27
- Binney, J. & Tremaine, S. 1994, *Galactic Dynamics*, 1st edn. (Princeton, USA: Princeton University Press)
- Birnboim, Y. & Dekel, A. 2003, *MNRAS*, 345, 349
- Bosma, A. 1978, PhD thesis, PhD Thesis, Groningen Univ., (1978)
- Bothun, G., Impey, C., & McGaugh, S. 1997, *PASP*, 109, 745
- Bournaud, F., Elmegreen, B. G., & Elmegreen, D. M. 2007, *ApJ*, 670, 237
- Bournaud, F., Elmegreen, B. G., & Martig, M. 2009, *ApJL*, 707, L1
- Brinks, E. & Klein, U. 1988, *MNRAS*, 231, 63P
- Brook, C. B., Governato, F., Roškar, R., et al. 2011, *MNRAS*, 415, 1051
- Brosch, N., Almoznino, E., & Hoffman, G. L. 1998, *A&A*, 331, 873
- Brüms, R. C. & Kroupa, P. 2012, *A&A*, 547, A65
- Cairós, L. M., Vílchez, J. M., González Pérez, J. N., Iglesias-Páramo, J., & Caon, N. 2001, *ApJS*, 133, 321
- Cannon, J. M., McClure-Griffiths, N. M., Skillman, E. D., & Côté, S. 2004, *ApJ*, 607, 274
- Cannon, J. M., Most, H. P., Skillman, E. D., et al. 2011, *ApJ*, 735, 36
- Caon, N., Cairós, L. M., Aguerra, J. A. L., & Muñoz-Tuñón, C. 2005, *ApJS*, 157, 218
- Casertano, S. 1983, *MNRAS*, 203, 735
- Cayatte, V., van Gorkom, J. H., Balkowski, C., & Kotanyi, C. 1990, *AJ*, 100, 604
- Cignoni, M. & Tosi, M. 2010, *Advances in Astronomy*, 2010
- Ciotti, L. 1991, *A&A*, 249, 99
- Ciotti, L. & Bertin, G. 1999, *A&A*, 352, 447

- Courteau, S., Cappellari, M., de Jong, R. S., et al. 2013, ArXiv e-prints
- Cox, A. L., Sparke, L. S., Watson, A. M., & van Moorsel, G. 2001, *AJ*, 121, 692
- Dalcanton, J. J., Williams, B. F., Seth, A. C., et al. 2009, *ApJS*, 183, 67
- de Blok, W. J. G. & McGaugh, S. S. 1996, *ApJL*, 469, L89
- de Blok, W. J. G., McGaugh, S. S., & Rubin, V. C. 2001, *AJ*, 122, 2396
- de Blok, W. J. G., McGaugh, S. S., & van der Hulst, J. M. 1996, *MNRAS*, 283, 18
- de Boer, T. J. L., Tolstoy, E., Hill, V., et al. 2012, *A&A*, 544, A73
- de Vaucouleurs, G. 1948, *Annales d'Astrophysique*, 11, 247
- de Vaucouleurs, G. 1959, *Handbuch der Physik*, 53, 275
- Dekel, A. & Silk, J. 1986, *ApJ*, 303, 39
- Dellenbusch, K. E., Gallagher, III, J. S., & Knezek, P. M. 2007, *ApJL*, 655, L29
- Dellenbusch, K. E., Gallagher, III, J. S., Knezek, P. M., & Noble, A. G. 2008, *AJ*, 135, 326
- Dolphin, A. E. 2002, *MNRAS*, 332, 91
- Doublier, V., Caulet, A., & Comte, G. 1999, *A&AS*, 138, 213
- Drinkwater, M. J., Jones, J. B., Gregg, M. D., & Phillipps, S. 2000, *PASA*, 17, 227
- Ekta, B., Pustilnik, S. A., & Chengalur, J. N. 2009, *MNRAS*, 397, 963
- Elmegreen, B. G., Zhang, H.-X., & Hunter, D. A. 2012, *ApJ*, 747, 105
- Elmegreen, D. M., Elmegreen, B. G., Marcus, M. T., et al. 2009, *ApJ*, 701, 306
- Elson, E. C., de Blok, W. J. G., & Kraan-Korteweg, R. C. 2010, *MNRAS*, 404, 2061
- Elson, E. C., de Blok, W. J. G., & Kraan-Korteweg, R. C. 2013, *MNRAS*, 429, 2550
- Fall, S. M. & Efstathiou, G. 1980, *MNRAS*, 193, 189
- Famaey, B. & McGaugh, S. S. 2012, *Living Reviews in Relativity*, 15, 10
- Fellhauer, M. & Kroupa, P. 2002, *MNRAS*, 330, 642
- Ferguson, H. C. & Binggeli, B. 1994, *A&ARv*, 6, 67
- Ferrara, A. & Tolstoy, E. 2000, *MNRAS*, 313, 291
- Ferrarese, L., Côté, P., Jordán, A., et al. 2006, *ApJS*, 164, 334
- Förster Schreiber, N. M., Genzel, R., Bouché, N., et al. 2009, *ApJ*, 706, 1364
- Förster Schreiber, N. M., Genzel, R., Lehnert, M. D., et al. 2006, *ApJ*, 645, 1062
- Freeman, K. C. 1970, *ApJ*, 160, 811
- Frenk, C. S. & White, S. D. M. 2012, *Annalen der Physik*, 524, 507
- Gallagher, III, J. S. & Hunter, D. A. 1987, *AJ*, 94, 43
- Gatto, A., Fraternali, F., Read, J. I., et al. 2013, ArXiv e-prints
- Gavazzi, G., Donati, A., Cucciati, O., et al. 2005, *A&A*, 430, 411
- Genzel, R., Burkert, A., Bouché, N., et al. 2008, *ApJ*, 687, 59
- Gil de Paz, A. & Madore, B. F. 2005, *ApJS*, 156, 345
- Gil de Paz, A., Madore, B. F., & Pevunova, O. 2003, *ApJS*, 147, 29
- Governato, F., Brook, C., Mayer, L., et al. 2010, *Nature*, 463, 203

- Governato, F., Zolotov, A., Pontzen, A., et al. 2012, *MNRAS*, 422, 1231
- Graham, A. W. & Guzmán, R. 2003, *AJ*, 125, 2936
- Gunn, J. E. & Gott, III, J. R. 1972, *ApJ*, 176, 1
- Hilker, M., Infante, L., Vieira, G., Kissler-Patig, M., & Richtler, T. 1999, *A&AS*, 134, 75
- Hoffman, G. L., Brosch, N., Salpeter, E. E., & Carle, N. J. 2003, *AJ*, 126, 2774
- Hubble, E. 1926, *Contributions from the Mount Wilson Observatory / Carnegie Institution of Washington*, 324, 1
- Hubble, E. P. 1927, *The Observatory*, 50, 276
- Hunter, D. A. & Elmegreen, B. G. 2004, *AJ*, 128, 2170
- Hunter, D. A., Elmegreen, B. G., & van Woerden, H. 2001, *ApJ*, 556, 773
- Hunter, D. A., Ficut-Vicas, D., Ashley, T., et al. 2012, *AJ*, 144, 134
- Hunter, D. A., van Woerden, H., & Gallagher, J. S. 1999, *AJ*, 118, 2184
- Hunter, D. A., van Woerden, H., & Gallagher, III, J. S. 1996, *ApJS*, 107, 739
- Hunter, D. A., Wilcots, E. M., van Woerden, H., Gallagher, J. S., & Kohle, S. 1998, *ApJL*, 495, L47
- Hurley-Keller, D., Mateo, M., & Nemec, J. 1998, *AJ*, 115, 1840
- Izotov, Y. I. & Thuan, T. X. 1999, *ApJ*, 511, 639
- Izotov, Y. I. & Thuan, T. X. 2004, *ApJ*, 616, 768
- Jerjen, H. & Binggeli, B. 1997, in *Astronomical Society of the Pacific Conference Series*, Vol. 116, *The Nature of Elliptical Galaxies; 2nd Stromlo Symposium*, ed. M. Arnaboldi, G. S. Da Costa, & P. Saha, 239
- Johnson, M., Hunter, D. A., Oh, S.-H., et al. 2012, *AJ*, 144, 152
- Jore, K. P. 1997, PhD thesis, CORNELL UNIVERSITY
- Kauffmann, G., White, S. D. M., & Guiderdoni, B. 1993, *MNRAS*, 264, 201
- Kennicutt, R. C. & Evans, N. J. 2012, *ARA&A*, 50, 531
- Kent, S. M. 1987, *AJ*, 93, 816
- Kereš, D., Katz, N., Weinberg, D. H., & Davé, R. 2005, *MNRAS*, 363, 2
- Kobulnicky, H. A. & Skillman, E. D. 2008, *AJ*, 135, 527
- Komatsu, E., Dunkley, J., Nolta, M. R., et al. 2009, *ApJS*, 180, 330
- Kormendy, J. 1985, *ApJ*, 295, 73
- Kormendy, J. & Bender, R. 2012, *ApJS*, 198, 2
- Kormendy, J., Fisher, D. B., Cornell, M. E., & Bender, R. 2009, *ApJS*, 182, 216
- Kravtsov, A. 2010, *Advances in Astronomy*, 2010
- López-Sánchez, Á. R., Koribalski, B. S., van Eymeren, J., et al. 2012, *MNRAS*, 419, 1051
- Lundmark, K. 1926, *Arkiv for Matematik, Astronomi och Fysik*, 19, B8
- Lundmark, K. 1927, *Nova Acta Regiae Soc. Sci. Upsaliensis Ser. V*, 1
- Mac Low, M.-M. & Ferrara, A. 1999, *ApJ*, 513, 142
- Marlowe, A. T., Meurer, G. R., & Heckman, T. M. 1999, *ApJ*, 522, 183
- Martinsson, T. P. K., Verheijen, M. A. W., Westfall, K. B., et al. 2013, *A&A*, 557, A131
- Mateo, M. L. 1998, *ARA&A*, 36, 435

- Matthews, L. D. & Uson, J. M. 2008, *AJ*, 135, 291
- Mayer, L., Mastropietro, C., Wadsley, J., Stadel, J., & Moore, B. 2006, *MNRAS*, 369, 1021
- McGaugh, S. S. 2005, *ApJ*, 632, 859
- McGaugh, S. S. 2012, *AJ*, 143, 40
- McGaugh, S. S., Schombert, J. M., Bothun, G. D., & de Blok, W. J. G. 2000, *ApJL*, 533, L99
- McQuinn, K. B. W., Skillman, E. D., Cannon, J. M., et al. 2010a, *ApJ*, 721, 297
- McQuinn, K. B. W., Skillman, E. D., Cannon, J. M., et al. 2010b, *ApJ*, 724, 49
- McQuinn, K. B. W., Skillman, E. D., Dalcanton, J. J., et al. 2012, *ApJ*, 759, 77
- Meurer, G. R., Carignan, C., Beaulieu, S. F., & Freeman, K. C. 1996, *AJ*, 111, 1551
- Meurer, G. R., Staveley-Smith, L., & Killeen, N. E. B. 1998, *MNRAS*, 300, 705
- Micheva, G., Östlin, G., Bergvall, N., et al. 2013, *MNRAS*, 431, 102
- Milgrom, M. 1983, *ApJ*, 270, 371
- Moore, B., Lake, G., & Katz, N. 1998, *ApJ*, 495, 139
- Most, H. P., Cannon, J. M., Salzer, J. J., et al. 2013, *AJ*, 145, 150
- Navarro, J. F., Frenk, C. S., & White, S. D. M. 1996, *ApJ*, 462, 563
- Noeske, K. G., Iglesias-Páramo, J., Vílchez, J. M., Papaderos, P., & Fricke, K. J. 2001, *A&A*, 371, 806
- Noordermeer, E., van der Hulst, J. M., Sancisi, R., Swaters, R. A., & van Albada, T. S. 2005, *A&A*, 442, 137
- Oh, S.-H., de Blok, W. J. G., Brinks, E., Walter, F., & Kennicutt, Jr., R. C. 2011, *AJ*, 141, 193
- Okamoto, T., Frenk, C. S., Jenkins, A., & Theuns, T. 2010, *MNRAS*, 406, 208
- Ostriker, J. P. & Peebles, P. J. E. 1973, *ApJ*, 186, 467
- Ott, J., Stilp, A. M., Warren, S. R., et al. 2012, *AJ*, 144, 123
- Palunas, P. & Williams, T. B. 2000, *AJ*, 120, 2884
- Papaderos, P., Izotov, Y. I., Thuan, T. X., et al. 2002, *A&A*, 393, 461
- Papaderos, P., Loose, H.-H., Fricke, K. J., & Thuan, T. X. 1996a, *A&A*, 314, 59
- Papaderos, P., Loose, H.-H., Thuan, T. X., & Fricke, K. J. 1996b, *A&AS*, 120, 207
- Penny, S. J., Forbes, D. A., & Conselice, C. J. 2012, *MNRAS*, 422, 885
- Planck Collaboration. 2013, *ArXiv e-prints*
- Pustilnik, S. A., Brinks, E., Thuan, T. X., Lipovetsky, V. A., & Izotov, Y. I. 2001a, *AJ*, 121, 1413
- Pustilnik, S. A., Kniazev, A. Y., Lipovetsky, V. A., & Ugryumov, A. V. 2001b, *A&A*, 373, 24
- Putman, M. E., Bureau, M., Mould, J. R., Staveley-Smith, L., & Freeman, K. C. 1998, *AJ*, 115, 2345
- Ramya, S., Kantharia, N. G., & Prabhu, T. P. 2011, *ApJ*, 728, 124

- Salzer, J. J., Rosenberg, J. L., Weisstein, E. W., Mazzarella, J. M., & Bothun, G. D. 2002, *AJ*, 124, 191
- Sancisi, R. 2004, in *IAU Symposium*, Vol. 220, *Dark Matter in Galaxies*, ed. S. Ryder, D. Pisano, M. Walker, & K. Freeman, 233
- Sancisi, R., Fraternali, F., Oosterloo, T., & van der Hulst, T. 2008, *A&ARv*, 15, 189
- Sandage, A. & Binggeli, B. 1984, *AJ*, 89, 919
- Sandage, A., Binggeli, B., & Tammann, G. A. 1985, *AJ*, 90, 1759
- Sandage, A. & Hoffman, G. L. 1991, *ApJL*, 379, L45
- Sanders, R. H. 2010, *The Dark Matter Problem: A Historical Perspective*
- Sawala, T., Frenk, C. S., Crain, R. A., et al. 2013, *MNRAS*, 431, 1366
- Schaye, J., Dalla Vecchia, C., Booth, C. M., et al. 2010, *MNRAS*, 402, 1536
- Searle, L. & Sargent, W. L. W. 1972, *ApJ*, 173, 25
- Serra, P., Oosterloo, T., Morganti, R., et al. 2012, *MNRAS*, 422, 1835
- Sérsic, J. L. 1963, *Boletín de la Asociación Argentina de Astronomía La Plata Argentina*, 6, 41
- Silk, J., Wyse, R. F. G., & Shields, G. A. 1987, *ApJL*, 322, L59
- Simpson, C. E. & Gottesman, S. T. 2000, *AJ*, 120, 2975
- Simpson, C. E., Hunter, D. A., Nordgren, T. E., et al. 2011, *AJ*, 142, 82
- Skillman, E. D., Côté, S., & Miller, B. W. 2003, *AJ*, 125, 593
- Springel, V. & Hernquist, L. 2003, *MNRAS*, 339, 289
- Stil, J. M. & Israel, F. P. 2002, *A&A*, 392, 473
- Stringer, M. J., Bower, R. G., Cole, S., Frenk, C. S., & Theuns, T. 2012, *MNRAS*, 423, 1596
- Swaters, R. A., Sancisi, R., van Albada, T. S., & van der Hulst, J. M. 2009, *A&A*, 493, 871
- Swaters, R. A., Sancisi, R., van Albada, T. S., & van der Hulst, J. M. 2011, *ApJ*, 729, 118
- Swaters, R. A., van Albada, T. S., van der Hulst, J. M., & Sancisi, R. 2002, *A&A*, 390, 829
- Tammann, G. A. 1994, in *European Southern Observatory Conference and Workshop Proceedings*, Vol. 49, *European Southern Observatory Conference and Workshop Proceedings*, ed. G. Meylan & P. Prugniel, 3
- Taylor, C. L., Brinks, E., Grashuis, R. M., & Skillman, E. D. 1995, *ApJS*, 99, 427
- Taylor, C. L., Brinks, E., Pogge, R. W., & Skillman, E. D. 1994, *AJ*, 107, 971
- Taylor, C. L., Kobulnicky, H. A., & Skillman, E. D. 1998, in *Magellanic Clouds and Other Dwarf Galaxies*, ed. T. Richtler & J. M. Braun, 205–208
- Tegmark, M., Blanton, M. R., Strauss, M. A., et al. 2004, *ApJ*, 606, 702
- Telles, E. & Maddox, S. 2000, *MNRAS*, 311, 307
- Terlevich, R., Melnick, J., Masegosa, J., Moles, M., & Copetti, M. V. F. 1991, *A&AS*, 91, 285
- Thacker, R. J. & Couchman, H. M. P. 2001, *ApJL*, 555, L17

- Thuan, T. X., Hibbard, J. E., & Lévrier, F. 2004, *AJ*, 128, 617
- Tolstoy, E., Hill, V., & Tosi, M. 2009, *ARA&A*, 47, 371
- Tosi, M. 2004, *Memorie della Società Astronomica Italiana*, 75, 103
- Tosi, M., Greggio, L., Marconi, G., & Focardi, P. 1991, *AJ*, 102, 951
- Tully, R. B. & Verheijen, M. A. W. 1997, *ApJ*, 484, 145
- van Albada, T. S., Bahcall, J. N., Begeman, K., & Sancisi, R. 1985, *ApJ*, 295, 305
- van Albada, T. S. & Sancisi, R. 1986, *Royal Society of London Philosophical Transactions Series A*, 320, 447
- van der Kruit, P. C. & Freeman, K. C. 2011, *ARA&A*, 49, 301
- van Eymeren, J., Marcelin, M., Koribalski, B., et al. 2009a, *A&A*, 493, 511
- van Eymeren, J., Marcelin, M., Koribalski, B. S., et al. 2009b, *A&A*, 505, 105
- van Zee, L., Salzer, J. J., & Skillman, E. D. 2001, *AJ*, 122, 121
- van Zee, L., Skillman, E. D., & Salzer, J. J. 1998a, *AJ*, 116, 1186
- van Zee, L., Skillman, E. D., & Salzer, J. J. 1998b, *AJ*, 116, 1186
- van Zee, L., Westpfahl, D., Haynes, M. P., & Salzer, J. J. 1998c, *AJ*, 115, 1000
- Verheijen, M. A. W. 2001, *ApJ*, 563, 694
- Verheijen, M. A. W. & Sancisi, R. 2001, *A&A*, 370, 765
- Viallefond, F. & Thuan, T. X. 1983, *ApJ*, 269, 444
- Vogelsberger, M., Genel, S., Sijacki, D., et al. 2013, *ArXiv e-prints*
- Walter, F., Brinks, E., de Blok, W. J. G., et al. 2008, *AJ*, 136, 2563
- Walter, F., Brinks, E., Duric, N., & Klein, U. 1997, *AJ*, 113, 2031
- Warren, S. R., Weisz, D. R., Skillman, E. D., et al. 2011, *ApJ*, 738, 10
- Weisz, D. R., Dalcanton, J. J., Williams, B. F., et al. 2011, *ApJ*, 739, 5
- White, S. D. M. & Frenk, C. S. 1991, *ApJ*, 379, 52
- White, S. D. M. & Rees, M. J. 1978, *MNRAS*, 183, 341
- Wilcots, E. M. & Miller, B. W. 1998, *AJ*, 116, 2363
- Willman, B., Blanton, M. R., West, A. A., et al. 2005, *AJ*, 129, 2692
- Wirth, A. & Gallagher, III, J. S. 1984, *ApJ*, 282, 85
- Wolf, J., Martinez, G. D., Bullock, J. S., et al. 2010, *MNRAS*, 406, 1220
- Zucker, D. B., Belokurov, V., Evans, N. W., et al. 2006a, *ApJL*, 650, L41
- Zucker, D. B., Belokurov, V., Evans, N. W., et al. 2006b, *ApJL*, 643, L103
- Zwicky, F. & Zwicky, M. A. 1971, *Catalogue of selected compact galaxies and of post-eruptive galaxies*